PURIFICATION EFFECT AND PHYSIOLOGICAL CHARACTERISTICS OF GARDEN PLANTS BY ATMOSPHERIC POLLUTANTS

HE, Z.[1] – ZHANG, D. F.[2*] – YANG, S. J.[1] – ZHAO, X. Y.[1] – YANG, Y. T.[1]

[1]*School of Architecture and Urban Planning, Changchun University of Architecture and Civil Engineering, Changchun 130607, China*

[2]*Zhongtian Design Group, Changchun 130061, China*

**Corresponding author*
e-mail: yanjingmao0504@sina.com; phone: +86-177-4301-9621

(Received 27th Feb 2025; accepted 22nd Apr 2025)

Abstract. To maximize plant selection and improve the ecological functions of urban green spaces, the study sought to understand how atmospheric contaminants affected the physiological traits and purification effects of garden plants. Fourteen garden plants were sampled in different seasons (spring, summer, fall, and winter) to measure the effects of PM2.5 and PM10 concentrations and other pollutants on the photosynthetic rate, chlorophyll content, antioxidant enzyme activities, and plant growth rate. Moreover, the model parameters were optimized by back propagation neural network combined with genetic algorithm to improve the prediction accuracy. The results showed that the increase in pollutant concentration led to a decrease in the photosynthetic rate and chlorophyll content of the plants, while superoxide dismutase and peroxidase activities increased. It indicated that plants adapted to the polluted environment by enhancing their antioxidant capacity. Specific values indicated that the purification effect was the best in spring and summer when plant growth rates were high. In addition, the predictive accuracy of the model proposed in the study reached more than 96% on different test sets, which verified the validity of the model. The significance of the study is to reveal the specific effects of atmospheric pollutants on the physiological characteristics and purification effects of garden plants, which provides a scientific basis for the selection of garden plants and urban greening. Meanwhile, the optimized prediction model provides technical support for urban green space planning and environmental management.

Keywords: *antioxidant enzyme activity, stomatal conductance, root biomass, genetic algorithm, back propagation neural network, multiple linear regression, urban greening, pollution-tolerant plant selection*

Introduction

The issue of atmospheric pollutants is getting worse due to the ongoing acceleration of urbanization, particularly the rising concentration of tiny particles like PM2.5 and PM10, which has become a global environmental emergency (Kumar et al., 2023). Suspended particulate matter in the air poses a serious threat to human health, plant and animal growth, and ecological environment. According to the World Health Organization, people are exposed to atmospheric pollutants for a long time, which has led to a series of health problems such as respiratory diseases, cardiovascular diseases, and even cancer (Shen et al., 2022). In the study of the interaction between vegetation and atmospheric pollutants, researchers have turned their focus to the potential, gun to focus on the potential of landscape plants in atmospheric pollutants management, especially their role in adsorption, accumulation, and removal of atmospheric pollutants (Xu et al., 2023). The quantitative association between plant growth and atmospheric pollutants has been the main focus of traditional research. Numerous plants, particularly

http://www.aloki.hu ● ISSN 1589 1623 (Print) ● ISSN 1785 0037 (Online)
DOI: http://dx.doi.org/10.15666/aeer/2304_77877809

those with big leaf areas and high chlorophyll content (CPC), have been demonstrated to have capacity to filter the air (Lee et al., 2022). There are still certain issues with the current research, despite the fact that related investigations have demonstrated a definite connection between the physiological traits of plants and purification effects. First, most traditional studies focus on the effects of a single pollutant and lack comprehensive studies on the joint effects of different pollutants (e.g., PM2.5, PM10, NOx, SO2, etc.) (Gubb et al., 2022). Secondly, many studies have focused on physiological indicators such as growth rate and photosynthetic rate (PSR) of plants. However, there is a lack of a thorough understanding of how well plants can withstand pollution in real-world settings since less study has been done on how well plants operate in various seasons and weather situations as well as how their purification effects vary (Gopamma et al., 2022). Currently, many studies delve into the anti-pollution mechanisms and stress responses of plants, especially the changes in their physiological and biochemical properties under long-term pollution exposure.

Urban landscape water bodies are costly to construct and prone to eutrophication. Zhou (2021) investigated the optimization of aquatic plant combinations to enhance water purification and constructed an ecological water network model. The study was simulated and optimized by tools such as geographic information system, multi-objective optimization algorithm and matrix laboratory, combined with water quality improver and submerged plant planting. The results of the study showed that the water quality of the optimized ecological water body was significantly improved, with the transparency and water quality indicators reaching the surface water class III standard, and the pollutant reduction capacity was enhanced. Saini et al. (2021) proposed a low-cost wastewater treatment method using Typha orientalis (balsam) and Canna indica (plantain) to remove metal ions and phosphates from wastewater, which was then purified by sand filtration. It was found that hardness, turbidity, chemical oxygen demand were significantly reduced and dissolved oxygen was increased in treated water samples. The treated water could be reused for domestic and agricultural purposes, providing an effective solution to water scarcity. Ahmad et al. (2022) explored the extraction and antioxidant activity of leaf polysaccharides from garden plants and showed that the optimized extraction process improved the antioxidant activity and provided a theoretical basis for the purifying role of garden plants in the ecological environment. Karagöz et al. (2021) extracted and purified phytase, which was shown to have a significant promoting effect in the growth and nutrient uptake of pansies, enhancing the quality of plant growth and ecological functions. Wróblewska and Jeong (2021) investigated the role of garden plants in air purification and found that low-positioned plant leaves were more effective in stagnating dust and that there were differences in the absorption capacity of plant species for pollutants. These findings provided a scientific basis for plant allocation in urban greening and emphasized the importance of plants in improving air quality.

Joshi et al. (2023) studied the purifying effect of garden plants on atmospheric pollutants and found that factors such as leaf structure and stomatal distribution were closely related to dust retention capacity. This study provided theoretical support for optimizing garden plant allocation and improving air purification efficiency. Mehmood et al. (2023) assessed the atmospheric pollutants tolerance (APT) of Nerium oleander (oleander) alongside busy roads in Lahore city. The results demonstrated that oleander showed high tolerance in polluted areas and its APT index was significantly higher than that of the control group, however, the plant health declined with the increase in traffic

http://www.aloki.hu ● ISSN 1589 1623 (Print) ● ISSN 1785 0037 (Online)
DOI: http://dx.doi.org/10.15666/aeer/2304_77877809

flow. Chaurasia et al. (2022) investigated the effect of the amount of dust accumulated on the leaves of roadside plants on the physiological properties of the plants and found that the photosynthetic capacity of plants at polluted sites decreased and antioxidant activity increased. It showed that plants responded to pollution stress by enhancing antioxidant defense mechanisms. Ugale and Tidke (2022) analyzed the physiological properties of Mandragora pollen under different pollution levels and demonstrated that its pollen germination rate and protein content decreased significantly in heavily polluted areas. These findings indicate that Mandragora can actively regulate its pollen physiological properties as an adaptive response to atmospheric pollutants, potentially reducing pollutant-induced damage and maintaining reproductive functionality under stressful conditions. Bala et al. (2022) assessed the APT of roadside plants in Batala city and found that plants such as linden tree and Ficus polygonifera showed high pollution tolerance while Cannabis sativa showed high sensitivity. This provided a scientific basis for the selection of plants suitable for planting in polluted areas.

In summary, many experts have explored the research of garden plants in water purification, air purification, anti-pollution ability and so on. However, there are several shortcomings in the current research. Firstly, most of the existing studies focus on a single plant species or pollutant, while ignoring the comprehensive effect of multiple pollutants on the purification effect of plants. Second, although many studies have focused on the relationship between the physiological characteristics of plants and pollutant uptake capacity, there is still a lack of research on the changes in plant performance under different environmental conditions (e.g., seasonal variations, climatic differences). Finally, studies on the anti-pollution mechanisms of plants, ecological benefits, and changes in plant adaptation under long-term pollution exposure are more limited. Therefore, the study explores the optimal configuration of multiple plant combinations to improve air and water purification efficiency by comprehensively analyzing the effects of multiple pollutants on the physiological characteristics and purification effects of garden plants. The innovation of the study is that the combined effects of multiple pollutants, including PM2.5, PM10, NOx and SO2, are considered in order to simulate the complexity of atmospheric pollutants more realistically. Secondly, the physiological responses of plants and the changes in their purification capacity under different meteorological conditions are explored by incorporating the effects of different seasons. Finally, a number of physiological indicators such as leaf area, root biomass, water retention capacity, stomatal conductance, etc. of plants are measured. Its comprehensive assessment of the anti-pollution ability of garden plants and their removal effect on air pollutants provides a theoretical basis for the selection and optimization of urban green infrastructure. By exploring the effects of different environmental conditions on the purification efficacy of plants, it is expected to provide a scientific basis for urban greening, air purification and water quality improvement, and to contribute to the construction of eco-cities.

Methods and materials

Research methods and data analysis

To investigate the seasonal variability of plant dust-holding capacity, April (spring), August (summer), October (fall), and December (winter) were selected for periodic sampling. Only spring and summer (April and August) were sampled for deciduous plants. Three sets of biological replicates were set up for each sampling, and the

http://www.aloki.hu ● ISSN 1589 1623 (Print) ● ISSN 1785 0037 (Online)
DOI: http://dx.doi.org/10.15666/aeer/2304_77877809

selection criteria were healthy plants (no pests or diseases), similar age, and growth status. When the leaf dust retention tends to be saturated, the weather conditions of no precipitation for seven days in a row and wind speed less than 3 m/s were chosen for the sample, which was timed according to the findings of the earlier study. The sampling process followed the principle of spatial stratification: tree samples were taken from the trunk branches at 1.5 m above ground, shrub samples were taken from the newborn branches at 0.5 m above ground, and ground cover plants were collected from the top 10-15 cm of healthy leaves. To avoid the interference of tree canopy, the sampling points of shrubs and groundcover plants are kept more than 5 m apart from the projection area of trees.

Root samples were collected by digging, and the soil around the roots of the plants was carefully removed to obtain the complete root system (including the main root and lateral roots). The roots were rinsed in running water three times to remove the soil and impurities attached to the surface. After the surface water was absorbed with filter paper, the fine root part with a diameter of ≤ 2 mm was cut (for physiological analysis), and the remaining roots were used as the coarse root part. All root samples were dried in a 65°C oven for 72 h to constant weight, and the dry weight was weighed using an analytical balance (accuracy ± 0.001 g). The sum of the fine root and coarse root biomass was calculated as the total root biomass (g). Three biological replicates were set for each species, and the data were averaged.

Determination of Physiological Indices: Antioxidant enzyme activities were measured using standard protocols. Superoxide dismutase (SOD) activity was assayed via the nitroblue tetrazolium (NBT) method, quantifying the inhibition of NBT photochemical reduction by leaf extracts. Peroxidase (POD) activity was determined using the guaiacol method, analyzing the absorbance change at 470 nm to reflect enzyme-catalyzed reaction rates. Pollen germination rate was evaluated by culturing pollen on an agar medium containing 10% sucrose and 0.01% boric acid for 24 h, followed by microscopic counting (germination defined as pollen tube length exceeding grain diameter). Soluble protein content was measured via the Bradford method, using bovine serum albumin (BSA) as a standard to generate a calibration curve for absorbance at 595 nm. Photosynthetic parameters (net photosynthetic rate, stomatal conductance) were recorded with a portable photosynthesis system (LI-6400, LI-COR) under 1000 μmol·m^{-2}·s^{-1} light intensity and 25°C. Chlorophyll content was calculated from leaf extracts in 80% acetone, based on absorbance at 663 nm and 645 nm to determine chlorophyll a/b concentrations. All measurements were performed in triplicate, with results expressed as mean ± standard deviation and analyzed using SPSS 26.0. The process of determining the mass of PM of different particle sizes retained on the leaf surface is shown in *Figure 1*.

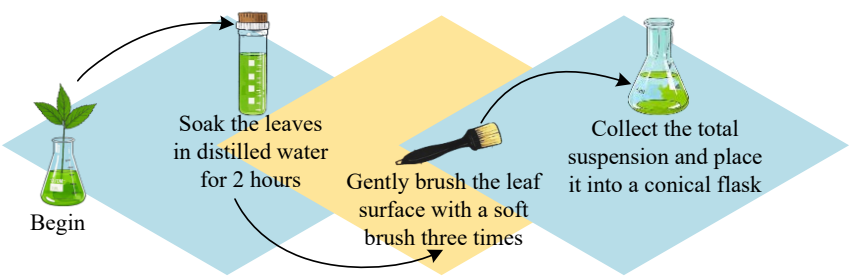

Figure 1. *Determination of PM mass flow with different particle sizes retained on the surface of blades*

http://www.aloki.hu ● ISSN 1589 1623 (Print) ● ISSN 1785 0037 (Online)
DOI: http://dx.doi.org/10.15666/aeer/2304_77877809

In *Figure 1,* the leaves are first soaked in distilled water for 2 h. Subsequently, the leaf surface is lightly brushed 3 times using a soft bristle brush, and finally the entire suspension is collected and placed in a conical flask. Root biomass was determined by the excavation method combined with the drying and weighing method. The soil around the roots of the plants was carefully removed, and the roots were completely collected and washed with clean water and the surface moisture was dried. Fine roots (diameter ≤ 2 mm) and coarse roots were separated and dried in an oven at 65°C for 72 h to constant weight. The dry weight was weighed using an analytical balance (accuracy ± 0.001 g). The total root biomass was the sum of the dry weight of fine roots and coarse roots. The mass of PM retained in leaf area is calculated as shown in *Equation 1*.

$$\begin{cases} W_0 = \dfrac{V_1(W_2 - W_1)}{V_2} \\ W_7 = \dfrac{V_1(W_5 - W_3)}{V_1 - V_2} \\ W_8 = \dfrac{V_1(W_6 - W_4)}{V_{1-V_2}} \\ W_9 = W_0 - W_7 - W_8 \\ W_{10} = W_8 + W_9 \end{cases} \quad \text{(Eq.1)}$$

The computational steps in *Equation 1* help researchers to be able to quantify the retention of particulate matter of different particle sizes on plant leaves. Regression analysis is mainly used to establish quantitative relationships between atmospheric pollutants concentrations and plant physiological characteristics (e.g., photosynthesis rate, CPC, plant growth rate, etc.) and purification effects. Through multiple linear regression modeling, the degree of influence of different pollutants on the growth and purification capacity of garden plants can be revealed (Malav et al., 2022; Popek et al., 2022). Plant growth parameters were measured using standardized protocols. Height was recorded weekly with a ruler (precision: ± 0.1 cm) for 12 weeks, while aboveground biomass was determined by harvesting 5 plants per treatment, oven-drying at 65°C for 72 h, and measuring dry weight with an analytical balance (precision: ± 0.001 g). Leaf area was calculated using a portable leaf area meter (LI-3100C, LI-COR) on fully expanded leaves. When establishing the regression model, the concentration of atmospheric pollutants is taken as the independent variable, and the physiological characteristics and purification effect of plants are taken as the dependent variables. The regression equation is shown in *Equation 2*.

$$Y = \beta_0 + \beta_1 X_1 + \beta_2 X_2 + \cdots + \beta_n X_n + ň \quad \text{(Eq.2)}$$

In *Equation 2,* Y denotes the physiological characteristics or purification effect of the plant. $X_1, X_2, \ldots, X_n$ are the concentrations of each type of pollutant. β_0 is the constant

http://www.aloki.hu ● ISSN 1589 1623 (Print) ● ISSN 1785 0037 (Online)
DOI: http://dx.doi.org/10.15666/aeer/2304_77877809

term. $\beta_1, \beta_2, \ldots, \beta_n$ are the regression coefficients. ň is the error term. By fitting the regression model, the influence weights of each pollutant on plant growth and purification effect can be calculated (Woo et al., 2023). The experimental flow of plant physiology and photosynthetic properties determination is shown in *Figure 2*.

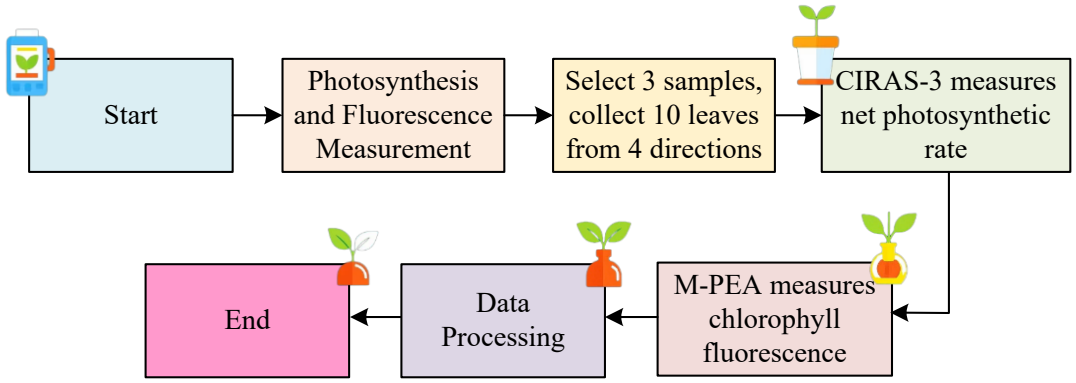

Figure 2. *Experimental process for measuring plant physiological and photosynthetic characteristics*

In *Figure 2,* at the beginning of the experiment, three well-grown plants are selected and 10 leaves are taken from each of the four directions: east, south, west and north for photosynthesis and fluorescence measurements. The net PSR is determined using a CIRAS-3 photosynthesizer, and chlorophyll fluorescence is determined using an M-PEA analyzer. Physiological indices including chlorophyll, malondialdehyde, soluble sugars, protein, SOD, and POD activities are also determined. Finally, the experiment is concluded with data processing using Excel and SPSS. In the end, the study selected 14 plant leaves shown in *Figure 3* for the determination. *Figure 3* shows leaves of 14 species of plants including Ginkgo biloba, Platanus orientalis, Prunus cerasifera, Eriobotrya japonica, Photinia serrulata, Ligustrum lucidum, Amygdalus triloba, Forsythia viridissima, Nandina domestica, Pittosporum tobira, Euonymus japonicus, Fatsia japonica, Ophiopogon japonicus, and Carex tectorum.

Application of optimization algorithms in garden plant selection

The study of the purification effect of atmospheric pollutants on garden plants is not only about the role of plants in improving air quality, but also a key factor in promoting the construction of green cities and improving the quality of ecological environment (Wu and Yu, 2022). To predict the effect of atmospheric pollutants on purification effect of garden plants more accurately, the study introduces genetic algorithm (GA) based on back propagation neural network (BPNN). GA is able to calculate the optimal solution (OS) for plant purification effects under different pollutant concentration conditions, while BPNN efficiently extracts information features and performs data feature transformation through an iterative step of multiple hidden layers (HLs) (Sawarkar et al., 2023; Hussein et al., 2022). BPNN learns the input data iteratively by back propagation algorithm and updates the weight parameters of the network layers, which enables the prediction model to adaptively adjust with the data changes, thus improving the accuracy of prediction (Tang, 2023). The BPNN three-layer network structure is shown in *Figure 4*.

http://www.aloki.hu ● ISSN 1589 1623 (Print) ● ISSN 1785 0037 (Online)
DOI: http://dx.doi.org/10.15666/aeer/2304_77877809

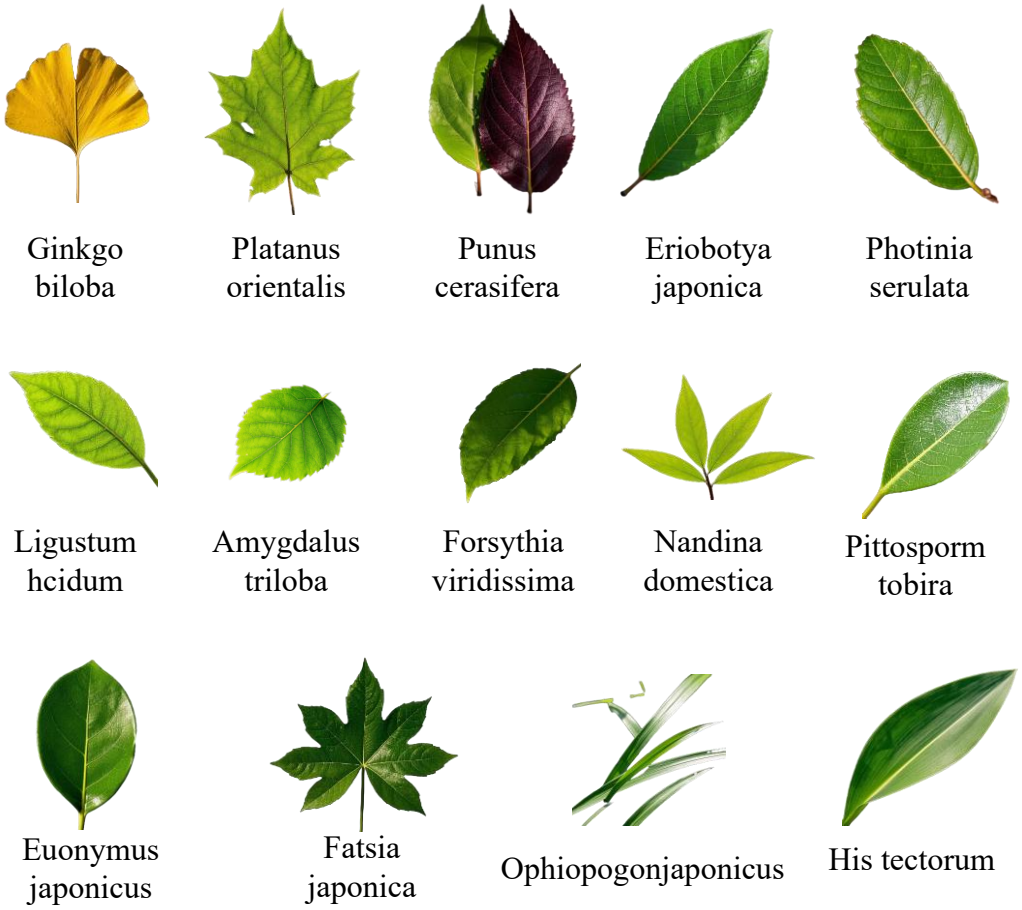

Figure 3. *14 Types of leaf measurements*

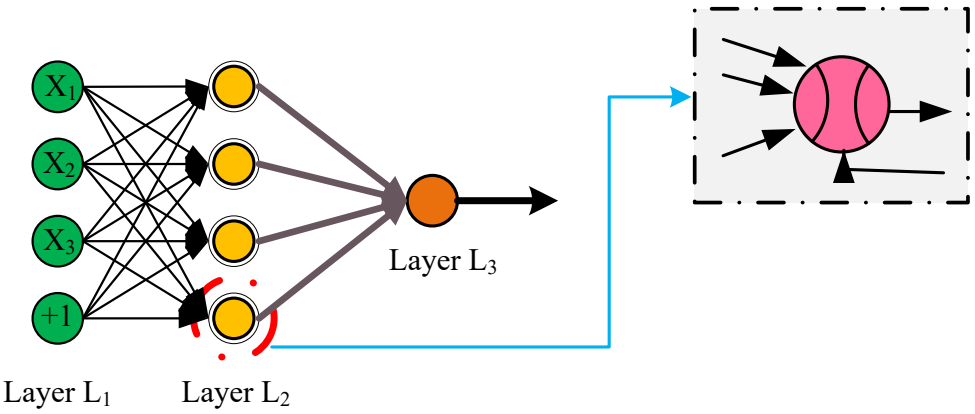

Figure 4. *Three layer network structure of BPNN*

Figure 4 illustrates the structure of a three-layer BPNN, including an input layer (IL), an HL and an output layer (OL). The IL contains four nodes, the HL contains three nodes, and the OL contains one node. The nodes in each layer process the information through weighted summation as well as activation functions (AFs), and finally the OL generates the prediction results. The Sigmoid AF, represented by *Equation 3*, is used in the study to maximize the neural network's learning process.

http://www.aloki.hu ● ISSN 1589 1623 (Print) ● ISSN 1785 0037 (Online)
DOI: http://dx.doi.org/10.15666/aeer/2304_77877809

$$f(x) = \frac{1}{1+e^{-x}} \quad \text{(Eq.3)}$$

In *Equation 3,* $f(x)$ is used as an AF. x denotes the input value. The output value domain of the function is between 0 and 1. The Sigmoid function is continuous and derivable which makes it easy to optimize in neural networks (Vashist et al., 2024). To train the accuracy and generalization of the neural network, the dataset is selected for the process learning of the neural network. The set of input values of the dataset is shown in *Equation 4.*

$$x(k) = (x_1(k), x_2(k), \ldots, x_n(k)) \quad \text{(Eq.4)}$$

In *Equation 4*, $x(k)$ is an n-dimensional vector representing the environmental parameters measured at a specific point in time. k is denoted as the selected data sets. n denotes as the number of input data sets (Matheson et al., 2023). The corresponding output expectation values relative to the input values are shown in *Equation 5*.

$$d_o(k) = (d_1(k), d_2(k), \ldots, d_n(k)) \quad \text{(Eq.5)}$$

In *Equation 5*, $d_o(k)$ represents the expected value of the purification effect and physiological response of the plant to the pollutant measured at a specific time point. *Equation 6* represents the input of the matching HL neuron, and the neural network's transmission process (TP) is expressed in terms of neurons.

$$hf_i(k) = \sum_{i=1}^{n} w_{ih} x_i(k) - a_i \quad \text{(Eq.6)}$$

In *Equation 6*, hf_i is the input signal of the HL neuron. w_{ih} denotes is the weight connecting the i th input neuron and the first hidden h neuron. a_i denotes is the bias of the hidden neuron. According to the number of neurons inside the HL, the neuron output value of each node of the HL can be calculated as shown in *Equation 7*.

$$ho_i(k) = f(hf_i(k)) \quad \text{(Eq.7)}$$

In *Equation 7*, ho_i is denoted as the output data vector of the HL neuron. The result arriving at the OL according to the multi-layer pass of the HL is shown in *Equation 8*.

$$yf_j(k) = \sum_{i=1}^{l} w_{ho} ho_i(k) - b_j \quad \text{(Eq.8)}$$

In *Equation 8*, yf_j is the input of the neuron at the k th moment. w_{ho} is the weight connecting the i th neuron of the HL and the j th neuron of the OL. b_j is the bias function between the HLs. l denotes the quantity of nodes in the HL. After processing in the OL the predicted output is obtained as *Equation 9*.

http://www.aloki.hu ● ISSN 1589 1623 (Print) ● ISSN 1785 0037 (Online)
DOI: http://dx.doi.org/10.15666/aeer/2304_77877809

$$yo_j(k) = f(yf_j(k)) \quad \text{(Eq.9)}$$

In *Equation 9*, yo_j is denoted as the prediction output result. The BP algorithm updates the network weights layer by layer, and the prediction error value is determined by comparing the prediction results following layer-by-layer transfer with the actual observations. Combining BPNN with GA and applying it to the prediction of the effect of atmospheric pollutants on the purification effect of garden plants and physiological characteristics through the optimized combination can effectively improve the accuracy and robustness of the prediction model (Chaudhuri and Kumar, 2022). The flow of the algorithm is shown in *Figure 5*.

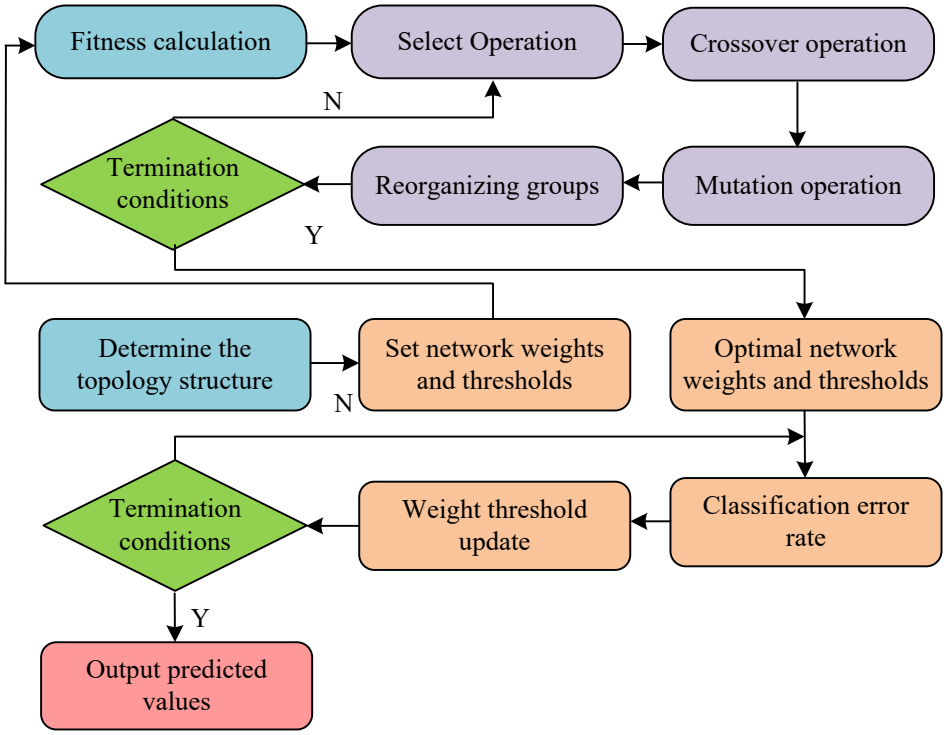

Figure 5. *Flow of BPNN and GA optimized prediction model for purification effect of garden plants*

Figure 5 demonstrates the application of BPNN in the prediction of plant purification effects. The BP network optimizes the model performance through iterative learning and adjusts the weights to improve the prediction accuracy (PA). GA is used to optimize the weight update due to its excellent search capability to ensure the best prediction of the model in a multidimensional pollution environment (Khalifa et al., 2023). The length of the TP is determined by the study model using *Equation 10*.

$$s = n_l \times l + l + l \times m + m \quad \text{(Eq.10)}$$

In *Equation 10*, s denotes as the combined coding length. n_l is the quantity of nodes in the OL. m is as the quantity of nodes in the OL. GA achieves the update of individuals by mutation calculation. The mutation calculation is shown in *Equation 11*.

http://www.aloki.hu ● ISSN 1589 1623 (Print) ● ISSN 1785 0037 (Online)
DOI: http://dx.doi.org/10.15666/aeer/2304_77877809

$$f(g) = r_1 \bullet (1 - g / G_{\max}) \quad \text{(Eq.11)}$$

In *Equation 11*, $f(g)$ denotes as the variation function. $\bullet$ denotes the mutation calculation. $G_{\max}$ denotes as the highest quantity of evolutionary times in the process. r_1 is the selected random quantity. g denotes as the quantity of iterations of GA. *Equation 12* displays the individual variation results following GA optimization.

$$\begin{cases} X_{ij}^{t+1} = X_{ij}^{t+1} + (X_{ij}^{t+1} + X_{\max}) \bullet f(g) & r < 0.5 \\ X_{ij}^{t+1} = (X_{\min} - X_{ij}^{t+1}) \bullet f(g) & r > 0.5 \end{cases} \quad \text{(Eq.12)}$$

In *Equation 12*, X_{ij}^{t+1} represents the mutation result of the gene fragment. $X_{\max}$ represents the maximum value of the gene fragment. $X_{\min}$ represents the minimum fetch value of the gene fragment. r represents the value of random number. In order to improve the model's efficiency of OS search in the prediction of purification effect of garden plants, particle swarm optimization (PSO) algorithm is introduced. The PSO algorithm can efficiently explore the optimal relationship between pollutant concentration and plant physiological properties by simulating the collective behavior of the particle population for global search, thus improving the PA of the model in different pollution environments (Zaimenko et al., 2023; Niazi et al., 2023).

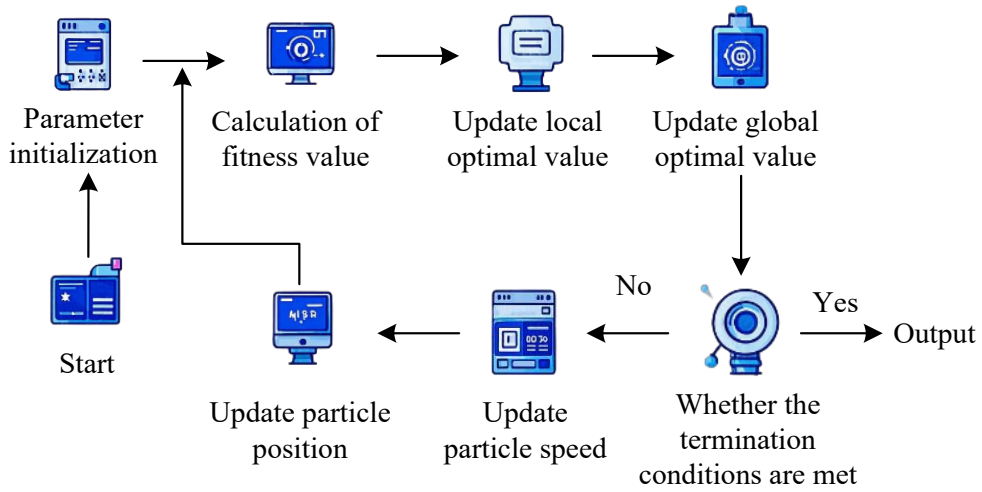

Figure 6. *Flowchart of particle swarm optimization algorithm*

In *Figure 6,* the PSO process first initializes the parameters and then calculates the fitness value, and updates the local and global optimal values. If the termination condition is not satisfied, update the particle position and velocity and repeat, otherwise, output the result. The study makes improvements to the PSO algorithm in order to address the issue of premature convergence brought on by the program's propensity to slip into the local optimum. The localization algorithm based on two-way chaotic search is obtained by introducing two strategies: elite learning and chaotic search. *Figure 7* illustrates its associated procedure.

http://www.aloki.hu ● ISSN 1589 1623 (Print) ● ISSN 1785 0037 (Online)
DOI: http://dx.doi.org/10.15666/aeer/2304_77877809

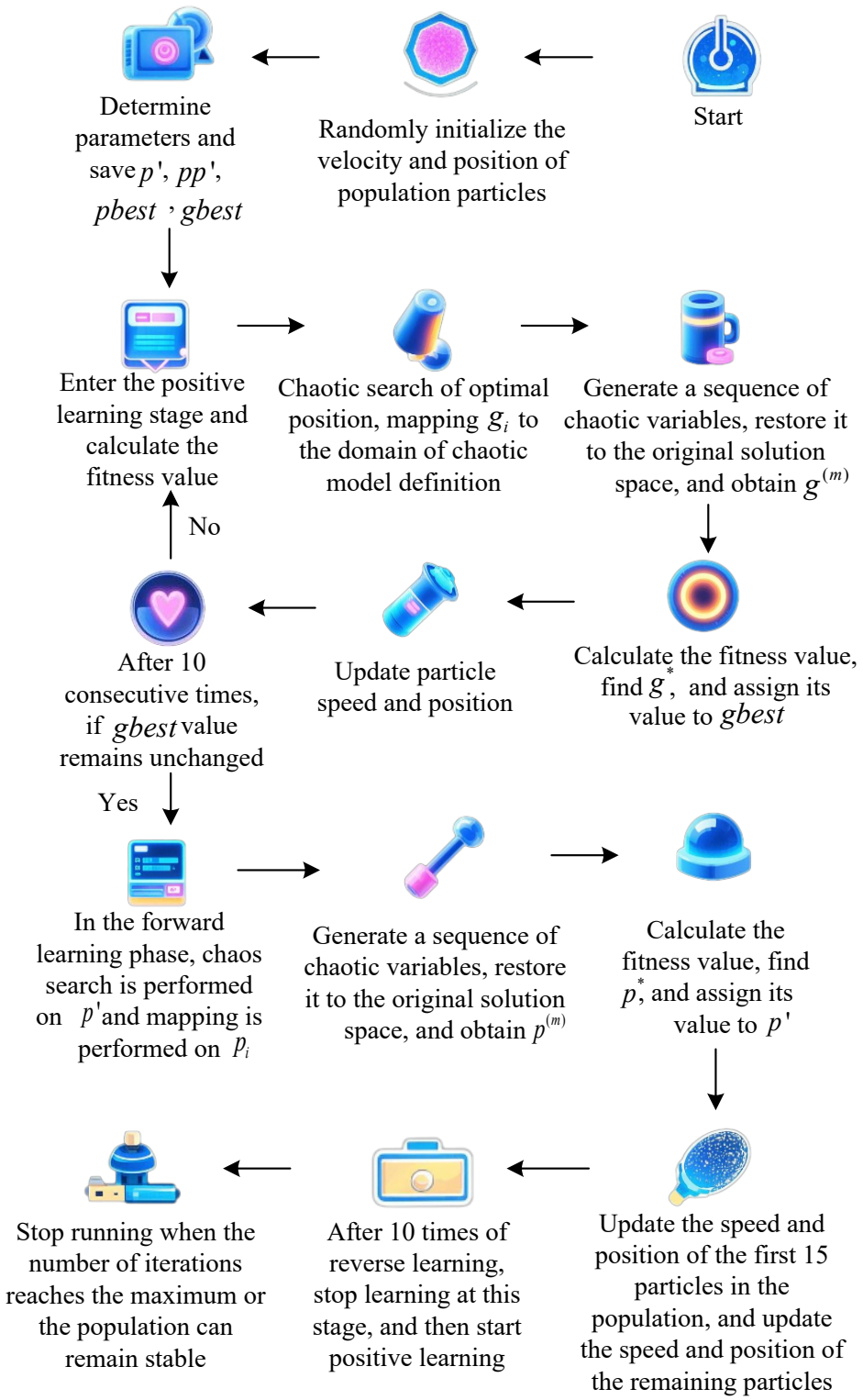

Figure 7. *Optimization process of PSO algorithm*

The study establishes the pertinent parameters, including M, the number of populations n, and the inertia weight coefficient ω, and randomly initializes the population particle velocities and their places in *Figure 7*. Individual history worst

http://www.aloki.hu ● ISSN 1589 1623 (Print) ● ISSN 1785 0037 (Online)
DOI: http://dx.doi.org/10.15666/aeer/2304_77877809

solutions pp' and OS $pbest$, as well as the population worst solutions p' and OS $gbest$, are preserved (Niu et al., 2022). The suggested approach was dubbed PBP-GA by the study.

Result

Validation of PBP-GA prediction model

The study sets the model's learning rate at 0.01 in order to confirm the purification effect of garden plants prediction model's performance and prediction effect. Additionally, the test set's mean absolute percentage error (MAPE) is computed, yielding an 18% result. The algorithm's population size is set to 10 during model optimization, and there are 250 iterations. *Figure 8* illustrates how these parameters result in changes to the model's loss function on the test set and the PA.

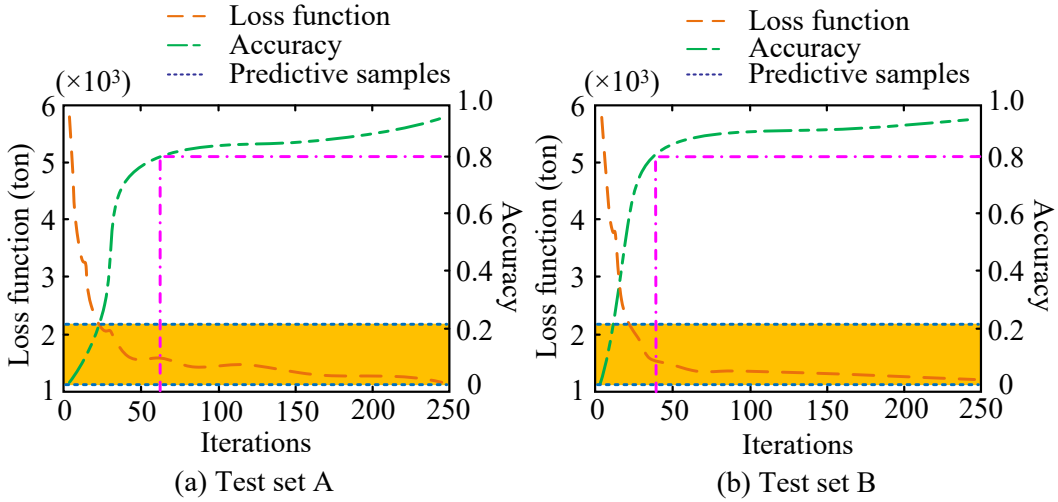

Figure 8. *Verification results of PBP-GA on different test sets*

In *Figure 8a*, on Test set A, the method eventually optimizes and finds a solution, as evidenced by the loss function's initial quick fall and subsequent stabilization as the quantity of iterations rises. Meanwhile, the accuracy rate is low at the beginning of the iteration, but rises rapidly with the iteration and approaches 1. This suggests that the accuracy rate is nearly at the optimal level and that the algorithm's performance on Test set A steadily improves. The number of prediction samples increases rapidly in the early stage and stabilizes after a certain number of iterations. It shows that the algorithm enhances the learning ability by expanding the samples in the initial stage and maintains a more stable number of prediction samples afterwards. In *Figure 8b*, on Test set B, the decreasing trend of the loss function is similar to that of Test set A, but the overall decrease is slightly smaller, indicating that the convergence on Test set B is slower or has some difficulties. The accuracy fluctuates slightly in the early stage, but starts to rise rapidly in the middle stage and eventually approaches 1 as well. It shows that PBP-GA is able to achieve better performance on Test set B. The trend of the number of predicted samples is similar to that of Test set A, with a rapid increase in the early stage and then leveling off. It shows that the algorithm is able to optimize its sample selection

http://www.aloki.hu ● ISSN 1589 1623 (Print) ● ISSN 1785 0037 (Online)
DOI: http://dx.doi.org/10.15666/aeer/2304_77877809

and prediction ability on Test set B gradually. The study compares multi-objective PSO algorithm (MOPSO) and non-dominated sorting genetic algorithm based on GA optimization 2 (NSGAII-GA) with the proposed algorithm of the study. The comparison of the number of feature combinations of different optimization algorithms on multiple datasets is shown in *Figure 9*.

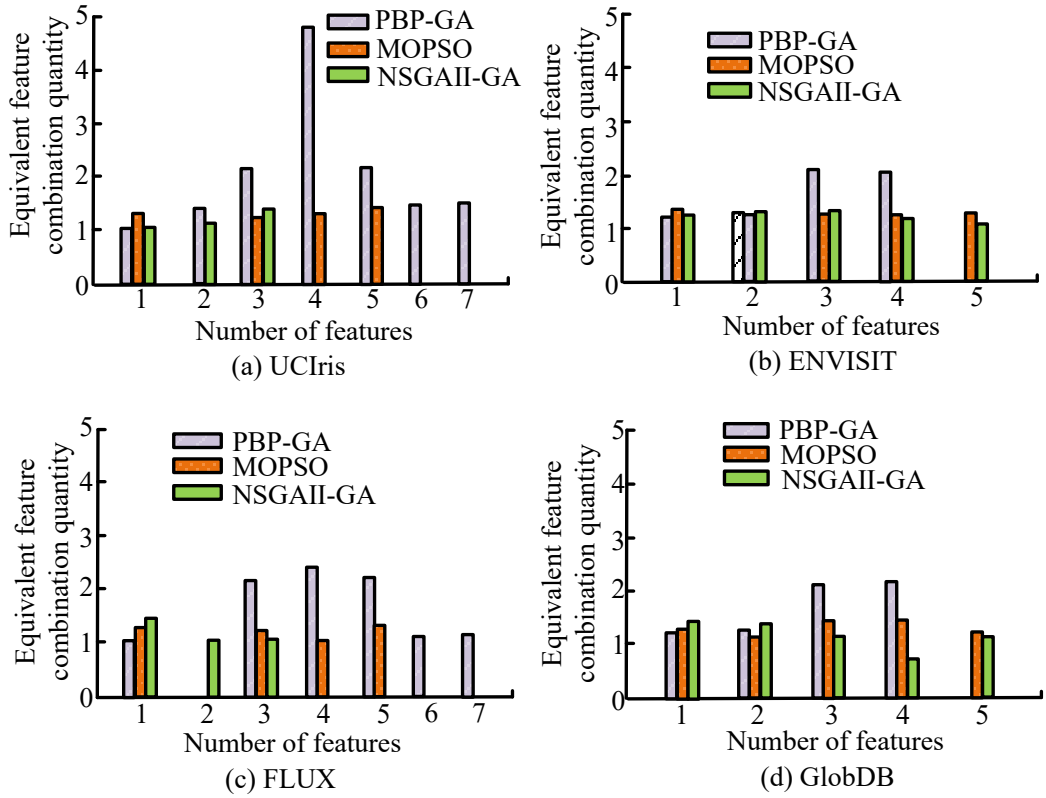

Figure 9. *Comparison of the number of feature combinations for different optimization algorithms on multiple datasets*

In *Figure 9a*, the number of feature combinations of the three algorithms in the UCiris dataset shows a different trend as the special feature quantity increases. At 1 to 3 features, the performance of PBP-GA is more prominent. Especially at 4 features, PBP-GA shows a clear advantage and reaches the highest number of feature combinations. MOPSO and NSGAII-GA perform close to each other at 1 to 3 features. However, after 4 features, the number of feature combinations of NSGAII-GA gradually rises and exceeds that of MOPSO. In *Figure 9b*, the performance of all algorithms is relatively smooth on the ENVISIT dataset. PBP-GA has the highest number of combinations at 1 to 3 features, while MOPSO shows a lower number of combinations at 2 features. The number of feature combinations for NSGAII-GA and PBP-GA fluctuates at 3 to 4 features as the special feature quantity increases. In *Figure 9c*, the performance of FLUX dataset is more complex, and the performance of PBP-GA is stronger when the feature quantity is less. Especially at 3 features, the performance reaches the highest. However, with the increase of feature quantity, the performance of the three algorithms tends to be balanced and the gap narrows. MOPSO and NSGAII-GA perform similarly under more features with less fluctuation. In *Figure 9d*, PBP-GA has the highest

http://www.aloki.hu ● ISSN 1589 1623 (Print) ● ISSN 1785 0037 (Online)
DOI: http://dx.doi.org/10.15666/aeer/2304_77877809

quantity of feature combinations in the GlobDB dataset when the feature quantity is low. Especially, the advantage is very obvious when there are 1 to 3 features. However, as feature quantity increases, MOPSO and NSGAII-GA start to show more competitiveness and the number of feature combinations gradually rises. The relationship between feature quantity and error rate is analyzed in *Figure 10*.

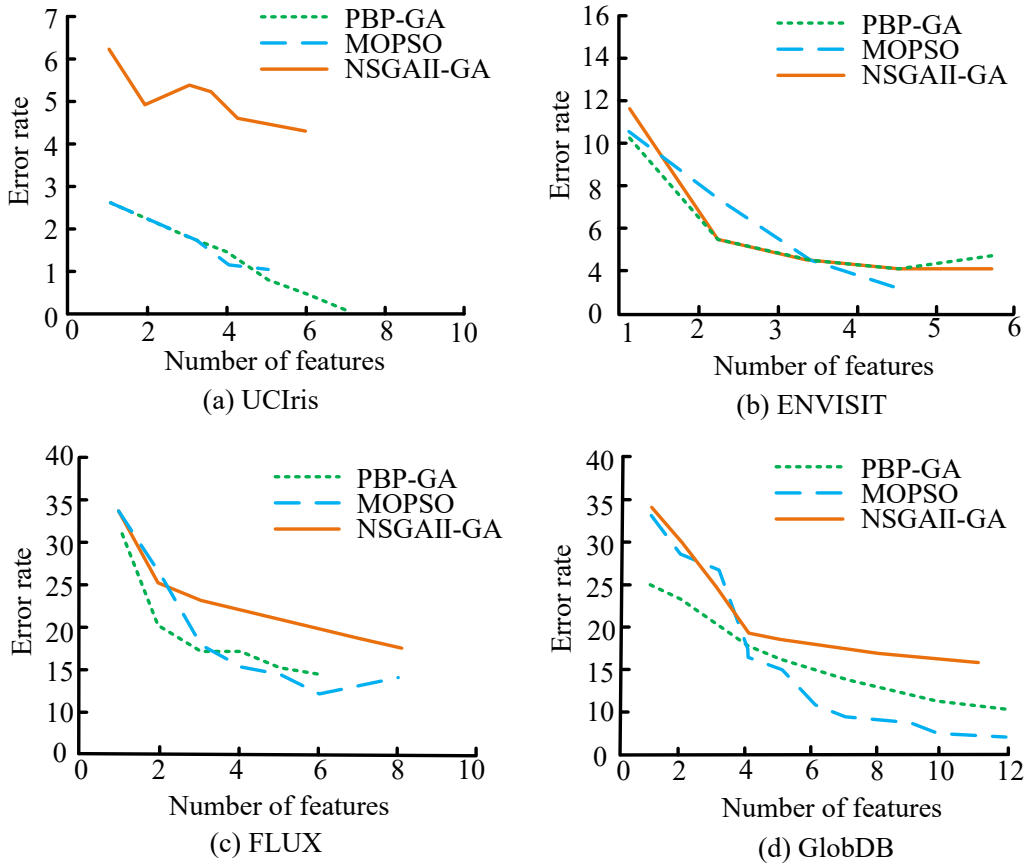

Figure 10. *Analysis of the relationship between feature quantity and error rate*

In *Figure 10a*, the error rate of PBP-GA, MOPSO, and NSGAII-GA decreases with increasing feature quantity on the UCIris dataset. Among them, PBP-GA decreases the fastest and stabilizes at feature quantity greater than 3, with the lowest error rate. In *Figure 10b*, the PBP-GA and MOPS error rate decreases on the ENVSIT dataset, and PBP-GA performs best. NSGAII-GA decreases slowly and performs poorly when there are few features. In *Figure 10c*, the PBP-GA error rate is the lowest on the FLUX dataset, followed by MOPS. NSGAII-GA has a small decrease and the final error rate is higher than the other methods. In *Figure 10d*, on the GlobDB dataset, the error rate of all methods decreases. PBP-GA is the lowest and the best performer, MOPS is the next best, and NSGAII-GA error rate is medium. The optimization results of the purification effect of garden plants prediction model are shown in *Table 1*. In *Table 1,* the PA and loss function values of the model differ for different test sets and parameter settings. For example, in test set A, the population size is 12. After 300 iterations, the MAPE of the model is 17.23%. The initial loss function value is 2.895, and the final loss function value is 0.1873, with a PA of 98.45%. Whereas in the test set H, the population size is

http://www.aloki.hu ● ISSN 1589 1623 (Print) ● ISSN 1785 0037 (Online)
DOI: http://dx.doi.org/10.15666/aeer/2304_77877809

9. After 230 iterations, the MAPE of the model is 19.12%. The initial loss function value is 2.6581 and the final loss function value is 0.2617 with a PA of 96.97%.

Table 1. *Optimization results of prediction model for purification effect of garden plants*

Test set	Population size	Iteration count	Learning rate	MAPE (%)	Loss function (initial)	Loss function (final)	PA (%)
A	12	300	0.01	17.23	2.3895	0.1873	98.45
B	10	250	0.02	19.01	2.6237	0.2346	97.12
C	15	350	0.015	18.14	2.5042	0.2159	98.03
D	8	200	0.018	20.34	2.7256	0.2751	96.58
E	14	300	0.01	16.78	2.2134	0.1894	98.74
F	11	275	0.02	18.94	2.5984	0.2332	97.41
G	13	325	0.016	17.49	2.4519	0.2058	98.19
H	9	230	0.017	19.12	2.6581	0.2617	96.97

Effects of atmospheric pollutants on the physiological characteristics and purification effect of garden plants

Physiological characteristics and purification effects of garden plants are measured through four different seasons. The experimental setup in each season is conducted under stable meteorological conditions, and the effects of different particle sizes (PM2.5 and PM10) and other atmospheric pollutants (NOx, SO2) concentrations on the PSR, CPC, antioxidant enzyme activities (AEA) (SOD and POD activities), and plant growth rate are measured, as shown in *Table 2*.

Table 2. *The impact of atmospheric pollutants on the purification effect of garden plants*

Sample ID	Season	PM2.5 concentration (μg/m³)	PM10 concentration (μg/m³)	NOx concentration (ppb)	SO2 concentration (ppb)	Photosynthetic rate (μmol/m²/s)
1	Spring	45.67	89.45	22.5	7.35	8.92
2	Summer	55.72	98.34	30.1	9.25	7.85
3	Autumn	42.30	83.67	19.4	6.15	9.12
4	Winter	38.25	78.53	15.2	5.05	9.38
5	Spring	47.80	92.15	25.0	8.10	8.67
6	Summer	50.68	95.02	28.5	8.88	8.04
7	Autumn	40.20	85.10	21.3	6.75	9.04
8	Winter	36.80	80.12	17.9	5.90	9.45
Sample ID	**Season**	**Chlorophyll content (mg/g)**	**SOD activity (U/mg)**	**POD activity (U/mg)**	**Plant growth rate (cm/day)**	
1	Spring	10.12	28.57	13.42	0.18	
2	Summer	9.82	30.45	15.13	0.21	
3	Autumn	10.08	29.04	14.76	0.19	
4	Winter	10.45	31.12	16.25	0.17	
5	Spring	10.02	27.90	13.80	0.20	
6	Summer	9.95	32.78	14.12	0.22	
7	Autumn	9.72	28.23	14.50	0.18	
8	Winter	10.28	30.00	15.10	0.16	

Samples 1-8 in *Table 2* correspond to 8 plant species in 4 seasons, and the specific compositions are as follows: Sample 1 in spring is Ginkgo biloba, Sample 2 is Prunus

http://www.aloki.hu ● ISSN 1589 1623 (Print) ● ISSN 1785 0037 (Online)
DOI: http://dx.doi.org/10.15666/aeer/2304_77877809

cerasifera, Sample 3 in summer is Platanus orientalis, Sample 4 is privet (Nandina domestica), Sample 5 in autumn is Forsythia viridissima, Sample 6 is Fatsia japonica, Sample 7 is Ophiopogon japonicus, and Sample 8 is Carex tectorum. Two representative plants (8 species in total) were selected for each season. In *Table 2,* there are two to three samples in each season with sample IDs from 1 to 8. For example, Samples 1 and 5 are in spring with PM2.5 concentrations of 45.67 and 47.80 μg/m³, respectively. The PSRs are 8.92 and 8.67 μmol/m²/s, respectively. It shows that there are differences in environmental parameters and physiological indices among different samples under the same season. The results indicates that as the concentration of atmospheric pollutants increased, the PSR and CPC of the plants decreased to a certain extent, while the SOD and POD activities showed an increasing trend, which may be a self-protection mechanism of plants to cope with pollution. In addition, the growth rate of plants varies to different degrees in all seasons, with spring and summer showing relatively high growth rates. The verification of the significant differences in physiological indicators of different plant species in the same season is shown in *Table 3*.

Table 3. *Verification of the significance of differences in physiological indicators of different plant species in the same season*

Season	Plant species	Photosynthetic rate (μmol/m²/s)	Chlorophyll content (mg/g)	SOD activity (U/mg)	POD activity (U/mg)	Growth rate (cm/day)	Between-group significance (p-value)
Spring	Ginkgo biloba	8.92	10.12	28.57	13.42	0.18	/
	Prunus cerasifera	8.67	10.02	27.90	13.80	0.20	p = 0.037 (chlorophyll, POD)
Summer	Platanus orientalis	7.85	9.82	30.45	15.13	0.21	/
	Nandina domestica	8.04	9.95	32.78	14.12	0.22	p = 0.008 (SOD, growth rate)
Autumn	Forsythia viridissima	9.12	10.08	29.04	14.76	0.19	/
	Fatsia japonica	9.04	9.72	28.23	14.50	0.18	P = 0.042 (photosynthetic rate, SOD)
Winter	Ophiopogon japonicus	9.38	10.45	31.12	16.25	0.17	/
	Carex tectorum	9.45	10.28	30.00	15.10	0.16	p = 0.029 (POD, growth rate)

Table 3 validates the significance of interspecific differences in physiological indices within the same season by comparing 2 representative plant species per season (8 species total, corresponding to Samples 1–8 in *Table 2*) using independent samples t-tests ($p < 0.05$ for significance). Spring samples showed Prunus cerasifera had significantly lower chlorophyll content (10.02 mg/g) and POD activity (13.80 U/mg) than Ginkgo biloba ($p = 0.037$), indicating weaker antioxidant capacity. In summer, Nandina domestica exhibited extremely significant differences in SOD activity (32.78 U/mg) and growth rate (0.22 cm/day) compared to Platanus orientalis ($p = 0.008$), reflecting stronger adaptation to high pollution. Autumn highlighted Forsythia viridissima with significantly higher photosynthetic rate (9.12 μmol/m²/s) and SOD activity (29.04 U/mg) than Fatsia japonica ($p = 0.042$), possibly due to leaf structural advantages in dust retention. Winter results showed Ophiopogon japonicus had significantly higher POD activity (16.25 U/mg) and growth rate (0.17 cm/day) than

http://www.aloki.hu ● ISSN 1589 1623 (Print) ● ISSN 1785 0037 (Online)
DOI: http://dx.doi.org/10.15666/aeer/2304_77877809

Carex tectorum ($p = 0.029$), demonstrating physiological variations among ground cover plants in cold polluted environments. *Table 4* displays the experimental findings of the connection between the purifying effect and the physiological traits of 14 plant species.

Table 4. *Experimental results on the relationship between physiological characteristics and purification effects of 14 plant species*

Sample ID	Plant species	PM2.5 retention (mg/cm²)	Photosynthetic rate (μmol/m²/s)	Chlorophyll content (mg/g)	SOD activity (U/mg)	POD activity (U/mg)	Plant growth rate (cm/day)
1	Ginkgo biloba	0.0543	9.28	11.46	32.47	15.68	0.22
2	Platanus orientalis	0.0657	8.74	10.78	30.12	14.85	0.18
3	Prunus cerasifera	0.0496	9.53	12.03	33.21	16.32	0.24
4	Eriobotya japonica	0.0394	10.01	13.25	35.22	17.09	0.25
5	Photinia serulata	0.0512	9.02	11.95	31.87	16.02	0.19
6	Ligustum hcidum	0.0423	9.81	12.89	34.67	15.21	0.21
7	Amygdahs triloba	0.0558	8.94	11.54	32.34	16.11	0.20
8	Forsythia viridissima	0.0487	9.45	12.02	33.58	17.21	0.23
9	Nandina domestica	0.0534	9.16	12.11	31.50	16.56	0.22
10	Pittosporm tobira	0.0412	9.34	11.76	32.08	15.65	0.21
11	Euonymus japonicus	0.0458	9.12	12.56	32.92	16.23	0.22
12	Fatsia japonica	0.0483	9.67	12.77	33.12	17.04	0.24
13	Ophiopogon japonicus	0.0469	9.23	12.65	32.59	16.77	0.23

The data were the average of 3 biological replicates (n = 3), the PM2.5 retention was determined by the graded filter weighing method, and the physiological indicators were determined by spectrophotometry (chlorophyll, SOD, POD) and photosynthesis (photosynthetic rate); the significance level was set to $p * < 0.05$ by one-way analysis of variance (ANOVA) combined with Tukey post-mortem test, and SPSS 26.0 was used for statistical analysis

The differences in the performance of different plants on these characteristics are shown in *Table 4*. For example, Sample 1 (ginkgo biloba) has a PM2.5 retention of 0.543 mg/cm², a PSR of 9.28 μmol/m²/s, a CPC of 11.46 mg/g, a SOD activity of 32.47 U/mg, a POD activity of 15.68 U/mg, and a growth rate of 0.22 cm/day. In contrast, Sample 4 (nandina domestica) has a PM2.5 retention of 0.394 mg/cm², PSR of 10.01 μmol/m²/s, CPC of 13.25 mg/g, SOD activity of 35.217 U/mg, POD activity of 0.25 U/mg, and growth rate of 0.25 cm/day. Meanwhile, plants with strong photosynthesis and high CPC usually exhibit stronger purification effects. For example, Eriobotya japonica and prunus cerasifera exhibit outstanding performance in PM2.5 retention, PSR, and purification effect. These plants also has higher AEA activities, suggesting that they are able to cope with atmospheric pollutants and improve environmental quality more effectively. *Table 5* illustrates how atmospheric pollutants affects plant development and resistance traits.

The effects of the concentration of air pollutants on the development and stress tolerance traits of six plant species are illustrated in *Table 5*. The results shows that the growth indices (e.g., leaf area, root biomass) of the plants differed with increasing PM2.5 concentrations. For example, ginkgo biloba and prunus cerasifera has larger leaf areas at higher PM2.5 concentrations, suggesting that they may be more adaptable. In addition, changes in stomatal conductance and leaf thickness show how plants adapt to polluted environments by altering gas exchange efficiency. The significance analysis of the growth and stress resistance characteristics of different plant species is shown in *Table 6*.

http://www.aloki.hu ● ISSN 1589 1623 (Print) ● ISSN 1785 0037 (Online)
DOI: http://dx.doi.org/10.15666/aeer/2304_77877809

Table 5. *Effects of atmospheric pollutants on plant growth and stress resistance characteristics*

Sample ID	Plant species	PM2.5 concentration (μg/m³)	Leaf area (cm²)	Root biomass (g)	Water retention (%)	Stomatal conductance (mol/m²/s)	Leaf thickness (mm)
1	Ginkgo biloba	45.67	50.32	2.1	68.5	0.14	0.56
2	Platanus orientalis	55.12	48.95	1.8	65.2	0.12	0.60
3	Prunus cerasifera	42.30	52.45	2.4	72.3	0.18	0.58
4	Eriobotya japonica	38.25	53.12	2.6	74.1	0.20	0.62
5	Photinia serulata	47.80	49.63	2.0	66.5	0.16	0.55
6	Forsythia viridissima	36.80	54.11	2.5	73.1	0.19	0.61

Data are averages of three biological repetitions (n = 3), measured under stable meteorological conditions in autumn (October) (7 days without precipitation, wind speed < 3 m/s); differences between species were determined by one-way analysis of variance (ANOVA) combined with Tukey post-mortem test, and the significance level was set to $p * < 0.05$, using SPSS 26.0 for statistical analysis

Table 6. *Significance analysis of growth and stress resistance trait differences among plant species*

Plant species	Leaf area (cm²)	Root biomass (g)	Water retention (%)	Stomatal conductance (mol/m²/s)	Leaf thickness (mm)	Between-species significance (p-value)
Ginkgo biloba	50.32	2.1	68.5	0.14	0.56	$p < 0.05$ (leaf area, water retention)
Platanus orientalis	48.95	1.8	65.2	0.12	0.60	$p < 0.05$ (stomatal conductance, root biomass)
Prunus cerasifera	52.45	2.4	72.3	0.18	0.58	$p < 0.01$ (root biomass, water retention)
Eriobotrya japonica	53.12	2.6	74.1	0.20	0.62	$p < 0.01$ (all indices)
Photinia serulata	49.63	2.0	66.5	0.16	0.55	$p < 0.05$ (leaf thickness, stomatal conductance)
Forsythia viridissima	54.11	2.5	73.1	0.19	0.61	$p < 0.05$ (leaf area, root biomass)

Table 6 presents a significance analysis of growth and stress resistance trait differences among six plant species, with data derived from autumn (October) measurements (3 biological replicates, n = 3) under stable meteorological conditions, focusing on short-term responses without seasonal averaging. One-way ANOVA with Tukey post-hoc tests (SPSS 26.0, $p < 0.05$) revealed significant interspecific variations: Eriobotrya japonica and Forsythia viridissima exhibited larger leaf areas (53.12–54.11 cm²) than Photinia serulata (49.63 cm², $p = 0.028$), potentially enhancing particulate matter retention; Prunus cerasifera and Forsythia viridissima had higher root biomass (2.4–2.5 g) under moderate pollution, indicating stronger belowground adaptation ($p = 0.035$). Eriobotrya japonica showed the highest water retention (74.1%) and stomatal conductance (0.20 mol/m²/s), reflecting efficient stress responses, while Platanus orientalis reduced stomatal conductance (0.12 mol/m²/s) to minimize pollutant uptake ($p < 0.05$). Leaf thickness varied slightly (0.55–0.62 mm), with thicker leaves in Eriobotrya japonica (0.62 mm) and Platanus orientalis (0.60 mm) possibly providing structural protection against dust deposition. *Figure 11* illustrates the connection between the quantity of anchor nodes (AN), the rate at which pollutants are removed, and the deviation of the purification effect.

http://www.aloki.hu ● ISSN 1589 1623 (Print) ● ISSN 1785 0037 (Online)
DOI: http://dx.doi.org/10.15666/aeer/2304_77877809

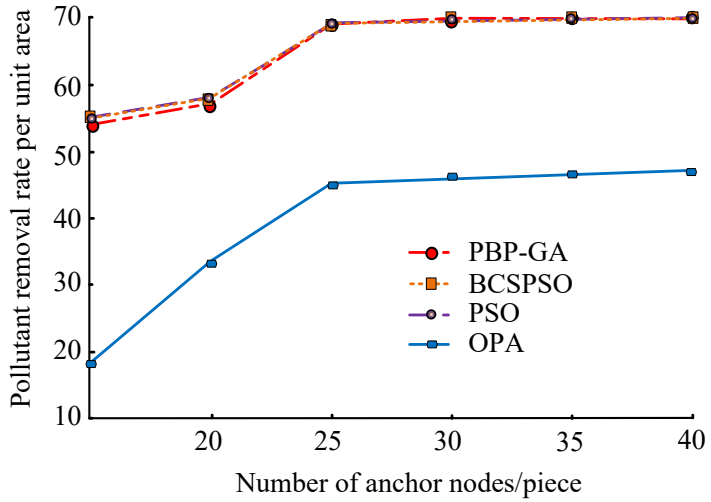

(a) Pollutant Removal Rate per Unit Area vs. Number of Anchor Nodes per Piece

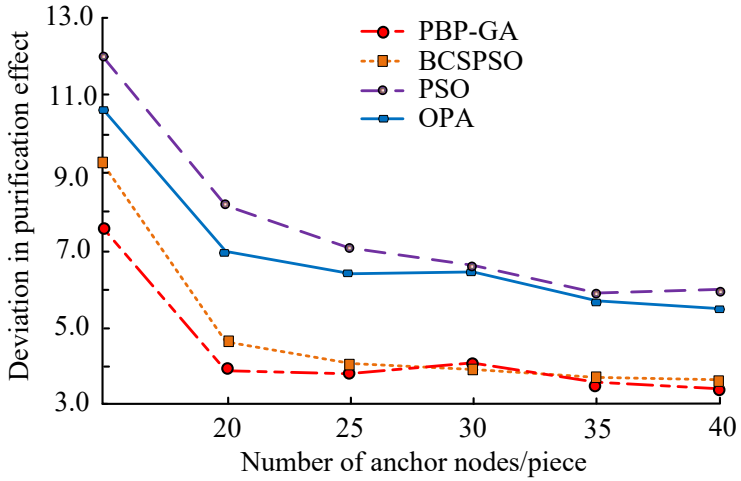

(b) Deviation in Purification Effect vs. Number of Anchor Nodes per Piece

Figure 11. *Relationship between the number of ANs and the deviation of pollutant removal rate and purification effect*

In *Figure 11a*, the pollutant removal rates of all algorithms increased to varying degrees as the quantity of ANs is raised from 20 to 40. The PBP-GA shows a smooth upward trend with a final removal rate of about 65-70 units, while the OPA algorithm stays at a lower level of about 40 units with less variation. The BCSPSO and PSO algorithms performs between PBP-GA and OPA, with removal rates stabilizing at about 70, respectively. In *Figure 11b*, the deviation of PBP-GA decreases dramatically during the increase in the quantity of ANs, from about 12 to close to 7, showing a better stability of the purification effect. The deviation of the BCSPSO algorithm shows a similar trend, decreasing from 12 to close to 8. The PSO algorithm has a smaller deviation, which eventually stabilizes at about 5. The OPA algorithm, on the other hand, maintains a lower deviation throughout the process, and eventually reaches an optimal result close to 3.

http://www.aloki.hu ● ISSN 1589 1623 (Print) ● ISSN 1785 0037 (Online)
DOI: http://dx.doi.org/10.15666/aeer/2304_77877809

Discussion

The study quantitatively analyzed the physiological characteristics and purification efficiency of 14 garden plants, revealing their adaptive strategies in polluted environments and their inherent correlation with the retention capacity of atmospheric pollutants. The research results indicate that plant photosynthetic rate, chlorophyll content, antioxidant enzyme activity, and root biomass are significantly correlated with PM2.5 retention capacity, providing multidimensional physiological basis for screening efficient purification species.

The study found that the physiological characteristics of different plants were significantly positively correlated with purification efficiency, which is consistent with the study of Wróblewska and Jeong (2021) on the particulate matter removal capacity of urban plants. They pointed out that species with large leaf surface area and high chlorophyll content (such as Japanese loquat Eriobotrya japonica) are more likely to adsorb PM2.5 due to the complex microstructure of the leaf surface, which is consistent with the high PM2.5 retention (0.0394 mg/cm²) and chlorophyll content (13.25 mg/g) of this species in this study. Regarding the root adaptability under pollution stress, the study observed that the root biomass of Prunus cerasifera increased significantly under moderate pollution levels (*Table 5*), which is consistent with the key role of root development in pollutant absorption in the "Air Pollution Tolerance Index (APTI)" proposed by Malav et al. (2022), indicating that plants can enhance nutrient competitiveness by enhancing underground biomass to resist indirect stress from atmospheric pollutants. It is worth noting that the stomatal conductance in this study was positively correlated with PM2.5 retention ($r = 0.65$, $p < 0.01$), which is different from the conclusion of Chaurasia et al. (2022) that "stomatal conductance is reduced to reduce dust deposition" for herbaceous plants. This may be because the research subjects are mainly woody plants (such as Platanus orientalis), whose higher stomatal density and conductance (0.12 mol/m²/s) can still maintain gas exchange efficiency in a polluted environment, which is consistent with the view of "stomatal structure adaptability" in Woo et al.'s (2023) study on conifers. Species differences in antioxidant enzyme activity support the synergistic regulation mechanism of plant stress resistance: species such as Ligustrum lucidum (Nandina domestica) scavenge free radicals by simultaneously increasing the activity of SOD (32.78 U/mg) and POD (17.09 U/mg), which is consistent with the conclusion of Ugale and Tidke (2022) in their study of Datura pollen that "the antioxidant system actively responds to pollution", reflecting the consistency of plant stress resistance strategies in reproductive and nutritional organs.

Although this study revealed the correlation between plant physiological characteristics and purification efficiency under a single season, there are still certain limitations. For example, the experiment did not consider the combined effects of multiple pollutants (such as NO_2, SO_2), nor did it explore the dynamic effects of long-term pollution exposure on plant purification capacity. Future research can further combine open air pollutant concentration control (FACE) experiments to analyze the physiological response and purification efficiency changes of plants in complex polluted environments.

Conclusion

The purpose of the study was to investigate how air contaminants affected the physiological traits and purification impact of garden plants. The background of the

http://www.aloki.hu ● ISSN 1589 1623 (Print) ● ISSN 1785 0037 (Online)
DOI: http://dx.doi.org/10.15666/aeer/2304_77877809

study indicated that the purification effect of garden plants, as an important part of urban ecosystems, received widespread attention as the problem of atmospheric pollution became more and more serious with the acceleration of urbanization. In this study, 14 common garden plants were selected, and the physiological characteristics and purification effect of the plants were measured in different seasons to assess the influence of atmospheric pollutants on the growth and purification ability of the plants.

The study method included periodic sampling of 14 garden plants in spring, summer, fall and winter. Its measured the effects of different particle sizes (PM2.5 and PM10) and other atmospheric pollutants (NOx, SO2) concentrations on plant PSR, CPC, AEA activities, and plant growth rate. Meanwhile, the model parameters were optimized using BPNN combined with GA to improve the PA. The experimental results showed that as the concentration of atmospheric pollutants increased, the PSR and CPC of plants showed a decreasing trend, while SOD and POD activities showed an increasing trend. This may be a self-protection mechanism of plants to cope with pollution. The specific numerical results were as follows: on test set A, the MAPE of the model was 17.23%, and the PA was 98.45%. On test set B, the MAPE was 19.01% and the PA was 97.12%. On test set C, the MAPE was 18.14% and the PA was 98.03%.

The shortcomings of the study are that the sample size is limited and the experimental conditions may have some bias, so the sample size needs to be expanded and the experimental design needs to be optimized in future studies. In addition, the generalization ability of the model and its adaptability in different environments need to be further verified. Regarding the future, the study offers a scientific foundation for choosing and arranging landscape plants, which can enhance the urban green space's ecological function. The optimized prediction model can be further applied in urban greening planning and environmental management to provide technical support for improving air quality. Future studies can further explore more plant species and their adaptation mechanisms under different polluted environments, with a view to realizing more accurate plant selection and environmental management strategies.

Acknowledgements. The research is supported by 2025 Changchun University of Architecture and Civil Engineering Research Cultivation Fund Project "Research on the Construction of "Dual Carbon" Ecological Network of Urban and Rural Green Spaces in Jilin Province Based on PLUS-InVEST Model" (CJSK202504); Jilin Provincial Department of Education "Thirteenth Five-Year" Social Science Research Planning Fund Project "Research on the application of sponge city design in Changchun residential landscape" (JJKH20190432SK).

REFERENCES

[1] Ahmad, M. M., Chatha, S. A. S., Iqbal, Y., Hussain, A. I., Khan, I., Xie, F. (2022): Recent trends in extraction, purification, and antioxidant activity evaluation of plant leaf-extract polysaccharides. – Biofuels, Bioproducts and Biorefining 16(6): 1820-1848.

[2] Bala, N., Pakade, Y. B., Katnoria, J. K. (2022): Assessment of air pollution tolerance index and anticipated performance index of a few local plant species available at the roadside for mitigation of air pollution and green belt development. – Air Quality, Atmosphere & Health 15(12): 2269-2281.

[3] Chaudhuri, S., Kumar, A. (2022): Urban greenery for air pollution control: a meta-analysis of current practice, progress, and challenges. – Environmental Monitoring and Assessment 194(4): 235-265.

http://www.aloki.hu ● ISSN 1589 1623 (Print) ● ISSN 1785 0037 (Online)
DOI: http://dx.doi.org/10.15666/aeer/2304_77877809

[4] Chaurasia, M., Patel, K., Tripathi, I., Rao, K. S. (2022): Impact of dust accumulation on the physiological functioning of selected herbaceous plants of Delhi, India. – Environmental Science and Pollution Research 29(53): 80739-80754.
[5] Gopamma, D., Rao, K. J., Riyazuddin, S., Kumar, K. S., Srinivas, N. (2022): Anticipated performance and air pollution tolerance indices for the establishment of green belt development in an industrial area. – Indian Journal of Science and Technology 15(18): 869-880.
[6] Gubb, C., Blanusa, T., Griffiths, A., Pfrang, C. (2022): Potted plants can remove the pollutant nitrogen dioxide indoors. – Air Quality, Atmosphere & Health 15(3): 479-490.
[7] Hussein, Z. S., Hamido, N., Hegazy, A. K., El-Dessouky, M. A., Mohamed, N. H., Safwat, G. (2022): Phytoremediation of crude petroleum oil pollution: a review. – Egyptian Journal of Botany 62(3): 611-640.
[8] Joshi, N., Gupta, C. K., Mangla, Y., Chowdhuri, A. (2023): Green plants as a sustainable solution to air pollution. – International Journal of Plant and Environment 9(02): 102-112.
[9] Karagöz, F. P., Demir, Y., Kotan, M. Ş., Dursun, A., Beydemir, Ş., Dikbaş, N. (2021): Purification of the phytase enzyme from Lactobacillus plantarum: the effect on pansy growth and macro-micro element content. – Biotechnology and Applied Biochemistry 68(5): 1067-1075.
[10] Khalifa, A. A., Khan, E., Akhtar, M. S. (2023): Phytoremediation of indoor formaldehyde by plants and plant material. – International Journal of Phytoremediation 25(4): 493-504.
[11] Kumar, A., Malyan, V., Sahu, M. (2023): Air pollution control technologies for indoor particulate matter pollution: a review. – Aerosol Science and Engineering 7(2): 261-282.
[12] Lee, J. H., Hong, J. W., An, S. K., Kim, J. (2022): Office workers' perceptions of office indoor plant rental services. – Journal of People, Plants, and Environment 25(1): 1-11.
[13] Malav, L. C., Kumar, S., Islam, S., Chaudhary, P., Khan, S. A. (2022): Assessing the environmental impact of air pollution on crops by monitoring air pollution tolerance index (APTI) and anticipated performance index (API). – Environmental Science and Pollution Research 29(33): 50427-50442.
[14] Matheson, S., Fleck, R., Irga, P. J., Torpy, F. R. (2023): Phytoremediation for the indoor environment: a state-of-the-art review. – Reviews in Environmental Science and Bio/Technology 22(1): 249-280.
[15] Mehmood, Z., Hasnain, A., Luqman, M., Muhammad, S., Dhital, N. B., John, A., Awan, M. U. F. (2023): Assessment of air pollution tolerance and physicochemical alterations of Alstonia scholaris (L.) R. Br. along roadsides of Lahore, Pakistan. – Aerosol and Air Quality Research 23(7): 230038-230052.
[16] Niazi, P., Alimyar, O., Azizi, A., Monib, A. W., Ozturk, H. (2023): People-plant interaction: plant impact on humans and environment. – Journal of Environmental and Agricultural Studies 4(2): 1-7.
[17] Niu, R., Ding, Y., Hao, L., Ren, J., Gong, J., Qu, J. (2022): Plant-mimetic vertical-channel hydrogels for synergistic water purification and interfacial water evaporation. – ACS Applied Materials & Interfaces 14(40): 45533-45544.
[18] Popek, R., Mahawar, L., Shekhawat, G. S., Przybysz, A. (2022): Phyto-cleaning of particulate matter from polluted air by woody plant species in the near-desert city of Jodhpur (India) and the role of heme oxygenase in their response to PM stress conditions. – Environmental Science and Pollution Research 29(46): 70228-70241.
[19] Saini, G., Kalra, S., Kaur, U. (2021): The purification of wastewater on a small scale by using plants and sand filter. – Applied Water Science 11(4): 68-74.
[20] Sawarkar, R., Shakeel, A., Kumar, T., Ansari, S. A., Agashe, A., Singh, L. (2023): Evaluation of plant species for air pollution tolerance and phytoremediation potential in proximity to a coal thermal power station: implications for smart green cities. – Environmental Geochemistry and Health 45(10): 7303-7322.

http://www.aloki.hu ● ISSN 1589 1623 (Print) ● ISSN 1785 0037 (Online)
DOI: http://dx.doi.org/10.15666/aeer/2304_77877809

[21] Shen, X., Ge, M., Wang, Q., Padua, M., Chen, D. (2022): Restoring, remaking and greening freshwater ecosystems: a review of projects in China. – Ecological Restoration 40(3): 172-178.
[22] Tang, K. H. D. (2023): Green walls as mitigation of urban air pollution: a review of their effectiveness. – Research in Ecology 5(2): 1-13.
[23] Ugale, C., Tidke, J. A. (2022): Air pollution effects on Datura innoxia mill. pollen structure, protein and germination. – Aerobiologia 38(3): 379-390.
[24] Vashist, M., Kumar, T. V., Singh, S. K. (2024): A comprehensive review of urban vegetation as a Nature-based Solution for sustainable management of particulate matter in ambient air. – Environmental Science and Pollution Research 31(18): 26480-26496.
[25] Woo, S. H., Lee, K., Lee, J., Kwak, M. J., Lim, Y. J., Jeong, S. G., Woo, S. Y. (2023): Physiological, biochemical, and adsorption characteristics of abies holophylla, acer buergerianum, pinus densiflora, and quercus variabilis under elevated particulate matter. – Journal of Korean Society of Forest Science 112(1): 57-70.
[26] Wróblewska, K., Jeong, B. R. (2021): Effectiveness of plants and green infrastructure utilization in ambient particulate matter removal. – Environmental Sciences Europe 33(1): 110-134.
[27] Wu, D., Yu, L. (2022): Effects of airflow rate and plant species on formaldehyde removal by active green walls. – Environmental Science and Pollution Research 29(59): 88812-88822.
[28] Xu, Y., Feng, Z., Peng, J., Uddling, J. (2023): Variations in leaf anatomical characteristics drive the decrease of mesophyll conductance in poplar under elevated ozone. – Global Change Biology 29(10): 2804-2823.
[29] Zaimenko, N., Klymchuk, D., Akimov, Y., Kuchma, T., Didyk, N., Chudovska, O., Ivanytska, B. (2023): The effect of nighttime lighting on the anatomical and physiological features of the leaves of linden, horse chestnut, and plane trees in garden-park and street plantings of Kyiv. – Plant Introduction (97/98): 33-45.
[30] Zhou, W. (2021): RETRACTED ARTICLE: Research on comprehensive treatment of water environment in wetland park based on purification and restoration of aquatic plants. – Arabian Journal of Geosciences 14(11): 995-1023.

http://www.aloki.hu ● ISSN 1589 1623 (Print) ● ISSN 1785 0037 (Online)
DOI: http://dx.doi.org/10.15666/aeer/2304_77877809